Constructing of highly porous thermoelectric structures with improved thermoelectric performance

Peilei He and Yue Wu (>>>)

Department of Chemical and Biological Engineering, Iowa State University, Ames, Iowa 50011, USA

© Tsinghua University Press and Springer-Verlag GmbH Germany, part of Springer Nature 2021 Received: 26 January 2021 / Revised: 12 April 2021 / Accepted: 1 May 2021

ABSTRACT

As more than 60% of worldwide consumed energy is unused and becomes waste heat every year, high-efficiency waste heat to power technologies are highly demanded for the conversion of wasted heat to electricity. Thermoelectrics which can convert the wasted heat directly into electricity represent a promising approach for energy recovery. Thermoelectric technology has existed for several decades, but its usage has been limited due to low efficiencies. Recent advances in nanotechnology have enabled the improving of thermoelectric properties which open up the thermoelectrics' feasibility in industry. In this paper, we present an overview of recent progress in increasing the porosity of thermoelectric materials from atomic scale to microscale, leading to the enhancement of figure of merit.

KEYWORDS

thermoelectrics, semiconductors, porous structures, thermal conductivity

Introduction

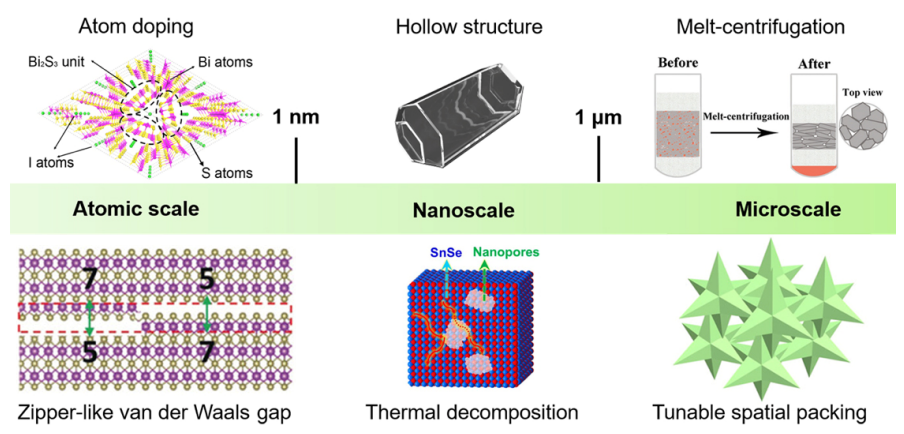
Due to the worldwide crises of energy shortage and environmental problems caused by the rapid development of human society, thermoelectric materials have attracted widespread research interest as a promising candidate to provide clean and renewable energy sources through converting the wasted heat into electricity [1-4]. Compared to conventional power generators which convert thermal energy into mechanical energy then to electrical energy, thermoelectrics own many advantages such as less noise, no pollution, no moving parts, and greater reliability [5, 6]. The performance of thermoelectric materials can be evaluated by a dimensionless figure of merit, $zT = S^2 \sigma T / \kappa$, where S is the Seebeck coefficient, σ is the electrical conductivity, T is the operational temperature, and κ is the thermal conductivity.

In the 1950s, Bi₂Te₃ was discovered as a thermoelectric material. And the basic science of thermoelectric materials was established, which was the first rapid development in thermoelectrics and launched the thermoelectrics industry [7]. Over the following three decades, no big development was achieved in the thermoelectric field [8], with Bi₂Te₃ compounds and its alloys remaining the best thermoelectric materials $(zT \approx 1)$ [9]. With a resurgence of interest in the early 1990s, there have been two primary approaches taken to develop the next generation of thermoelectric materials [8, 10, 11]. The first approach focuses on finding of new families of complex bulk materials which contained heavy-ion species with effective phonon-scattering centers [12, 13]. The other approach is using nanostructured materials systems. Compared with the same bulk materials, nanomaterials can significantly improve the thermoelectric figure of merit [10, 14, 15]. Regarding the approach of nanostructured thermoelectric materials, two ideas were dominant [8]. First, the quantum-confinement effects in nanomaterials could enhance the power factor $S^2\sigma$ [16]. Quantum mechanics provide a new route of designing thermoelectric materials. Second, the internal interfaces in nanostructures would be designed to reduce thermal conductivity, based on effectively scattering of phonons by the interfaces [17, 18]. Meanwhile, the interfaces have little effect on electrical conductivity because of the scattering lengths on electrons. Therefore, the lattice contribution to the thermal conductivity is independent of the electrical conductivity [19]. And more internal interfaces could be introduced by enhancing the porosity of the thermoelectric materials [20-22]. Therefore, using nanomaterials with high porosity, higher thermoelectric figure of merit would be obtained [23, 24]. This review focuses on recent studies on developing highly porous thermoelectric materials with enhanced properties. The increasing of porosity at different scales (Scheme 1) could optimize thermal transport and improve the thermoelectric performance. These may provide new insight to discover the new systems with excellent thermoelectric properties.

2 Atomic-scale porosity design for thermoelectric materials

At the atomic-scale level, two methods are used to increase the porosity of thermoelectric materials. The first method is introducing eco-friendly and cost-efficient element atoms (such as iodine and bromine) into the thermoelectric materials [25]. The doping of different atoms not only induced the enhancement of electric conductivity but also decreased the thermal conductivity because of the increased porosity. And these changes lead to the excellent figure of merit. The other method to increase porosity is breaking the lattice periodicity





Scheme 1 Different methods for increasing porosity at atomic-, nano-, and micro-scales.

by creating zipper-like van der waals (vdW) gap discontinuity [26]. In this method, low-temperature spark plasma sintering (SPS) is adopted to sinter nanoheterostructures to form monolith with zipper-like vdW gaps discontinuity. The existence of zipper-like vdW gaps can increase the porosity (16%) of this material which lead to the low lattice thermal conductivity and a high figure of merit.

2.1 Atom-doping

Dr. Wu and co-workers have introduced iodine (I, an ecofriendly and cost-efficient element) atoms into Bi₂S₃ structure and obtained higher zT than the pure metal sulfide thermoelectric materials [25]. First, potassium iodide as the I precursor was added into the typical solution-synthesized process of Bi₂S₃. Detailed structural characterizations confirmed that the crystal symmetry was changed to a more symmetric trigonal one (Bi₁₃S₁₈I₂) upon reconstruction of Bi₂S₃ (orthorhombic) (Figs. 1(a)-1(c)). The obtained $Bi_{13}S_{18}I_2$ nanorods showed lower thermal conductivity than the bulk structure and pure metal sulfide thermoelectric materials (Figs. 1(d) and 1(e)). The highest zT of 1.0 is achieved at 788 K which is much higher than bulk structure and other metal sulfides (Figs. 1(f) and 1(g)). And theoretical studies have been conducted to explore the origin of the excellent figure of merit. Aside from the high power factor induced by the beneficial electronic structure, the extremely low thermal conductivity was induced by the atomic structure of $Bi_{13}S_{18}I_2$. The insertion of I atom in Bi_2S_3 structure leads to the formation of disordered Bi(X) and open-framework which increased the porosity in the lattice level. They also introduced the bromine atom into Bi_2S_3 and synthesized analogous $Bi_{19}S_{27}Br_3$ with similar porous structure. Likewise, based on proper wet-chemical method, other open-framework with porous structure derived from metal chalcogenides, such as $Sn_2BiS_2I_3$ [27] and $Bi_{11}Se_{12}Cl_{19}$ [28], could be synthesized.

2.2 Lattice gap creating

Another method to increase porosity at atomic scale is breaking the lattice periodicity. Dr. Wu and co-workers synthesized PbTe-Bi₂Te₃ nanoheterostructures (NHSs) employing solution synthesis method [26]. Then low-temperature SPS is conducted to sinter the PbTe-Bi₂Te₃ NHSs to form nanostructured monolith of PbBi_{2n}Te_{1+3n} which was well characterized to study its composition and structure. Detailed structural analysis indicated the product could be indexed as PbBi₄Te₇ (Fig. 2(a)). And through adjusting the ratio of PbTe to Bi₂Te₃ in the NHS, PbBi₆Te₁₀ could also be obtained after sintering. Figure 2(b) shows the high-resolution transmission electron microscopy (HRTEM) image of focused-ion-beam-milled thin section which reveals abundant pores and nano-sized grains. High-angle

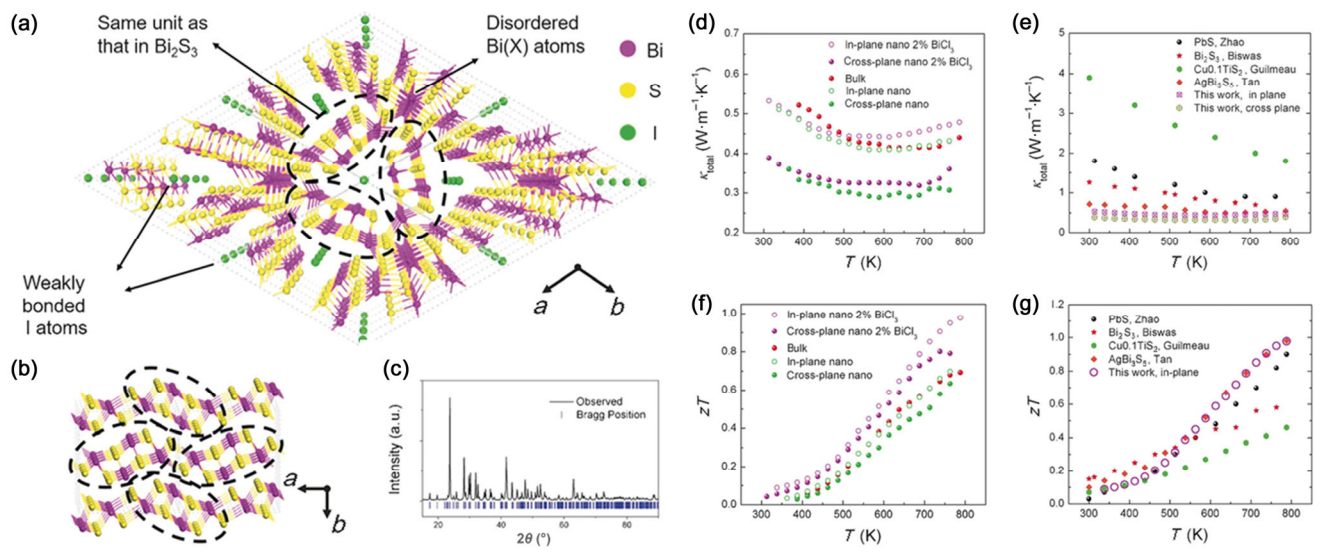


Figure 1 The crystal structure of (a) $Bi_{13}S_{18}I_2$ vs. (b) Bi_2S_3 . The dashed circles illustrate the inherited fragment in $Bi_{13}S_{18}I_2$ from Bi_2S_3 . (c) The powder X-ray diffraction (PXRD) profile of the bulk $Bi_{13}S_{18}I_2$. (d) and (e) Thermal conductivity of the nano $Bi_{13}S_{18}I_2$ and other reported metal sulfides. (f) Figure of merit, zT, of different $Bi_{13}S_{18}I_2$ samples. (g) Comparison zT of the nano $Bi_{13}S_{18}I_2$ with other metal sulfides. Reproduced with permission from Ref. [25], © Wiley-VCH Verlag GmbH & Co. KGaA, Weinheim 2018.

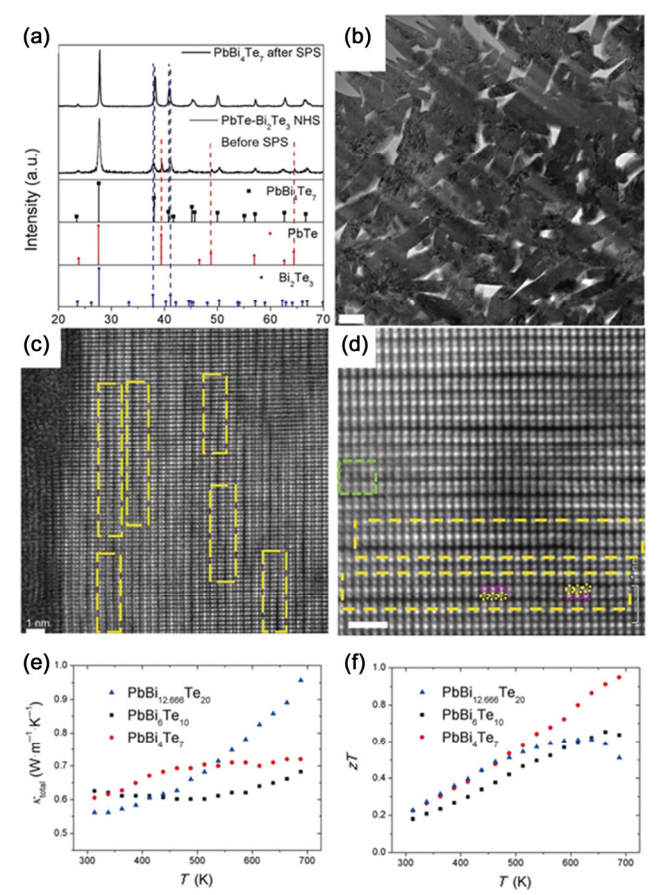


Figure 2 (a) XRD profiles of the 0.14286 PbTe-0.85714 Bi_{0.666}Te NHS before SPS and nano PbBi₄Te₇ sample after SPS. (b) HRTEM image of the nano PbBi₆Te₁₀ sample. Scale bar is 100 nm. HAADF-STEM images of nano PbBi₆Te₁₀ (c) and PbBi₄Te₇ (d) samples, respectively. Both scale bars are 1 nm. (e) Temperature-dependent of total thermal conductivity. (f) Figure of merit of all the samples. Reproduced with permission from Ref. [26], © Wiley-VCH Verlag GmbH & Co. KGaA, Weinheim 2018.

annular dark-field scanning transmission electron microscope (HAADF-STEM) images (Figs. 2(c) and 2(d)) of PbBi₄Te₇ and PbBi₆Te₁₀, periodical quintuple and septuple layers were observed. And inconsecutive gaps between the quintuple and septuple layers formed some zipper-like vdW gaps discontinuity as highlighted in the dashed yellow boxes. For the PbBi₄Te₇ sample, its porosity was calculated as 16% based on the relative density (84%). Therefore, these zipper-like vdW gaps can increase the porosity of final product and break the coherence of phonon transport which would decrease the thermal conductivity. The molecular dynamics (MD) simulations indicated that the break of coherence can reduce the thermal conductivity by 25% in the structure with zipper-like vdW gaps. And the nano PbBi₄Te₇ showed the lower thermal conductivity and the highest zTvalue (Figs. 2(e) and 2(f)). Similarly, through wet chemical and SPS method, the lattice periodicity in β-Ag₂Se was breaking and induced the formation high-density pores [29]. Due to the phonon scattering by the pores, an ultralow lattice thermal conductivity of $\sim 0.35~W \cdot m^{-1} \cdot K^{-1}$ at 300 K is obtained, resulting in a figure of merit, zT, of ~ 0.7 at 300 K.

Nano-scale pores construction for thermoelectric materials

Many different methods have been used to create nanoscale pores in the thermoelectric materials. Herein, some interesting methods were discussed. The first one is constructing hollow nanostructures and sintering them into pellet [30]. The second one is creating nanopores during the sintering process through decomposing partial composition of nanoprecipitates [31].

3.1 Hierarchical porous structures from assembling of hollow nanostructures

To further increase the porosity of a thermoelectric material, it might be an effective way to use hollow nanostructure as a powder precursor, as it intrinsically holds high porosity and a large amount of void spaces [32]. The existence of nanoscale cavities in nanostructures could decrease the lattice thermal conductivity obviously due to the scattering of phonons by the pores [20]. At the same time, there is no big difference in the electrical conductivity because of the large crystal grains. Therefore, an excellent zT was obtained simultaneously. Recently, Wu's group also constructed internally hollow structures with nanoscale cavities [30]. In the formation of Bi₂Te_{2.5}Se_{0.5} hollow nanorods, the mechanism of nanoscale Kirkendall effect based outward diffusion was used to produce the hollow nanostructures. First, Te solid nanorods formed in the wet-chemical process. Then Bi(NO₃)₃ were injected into the reaction system to form Te@Bi-Se core-shell nanorods. In the final step, Te(Se) and Bi react with and diffuse into each other to form the final hollow structure (Figs. 3(a)-3(c)). After sintering, the scanning electron microscopy (SEM) image of a focused-ion-beam (FIB) cut sample indicated that the sintered pellet was a highly porous material with larger grains (Fig. 3(d)). The relative density was 67.9% which is much lower than solid materials. And due to the phonon scattering by the nanopores, the thermal conductivity was decreased sharply (Fig. 3(e)). At the same time, the electric conductivity of porous BiTeSe material was still maintained quite high due to the larger grains and high crystallinity. Thus, a higher zT of 1.18 at 463 K has been obtained (Fig. 3(d)).

This approach can also be adopted to synthesize other porous thermoelectric chalcogenide materials and increase their thermoelectric performance. Aside from the satisfactory performance, hollow nanostructured thermoelectric materials have lower relative mass density which could endow them with better portability. Also, this hollow nanostructured approach could decrease the use of expensive raw materials.

3.2 Nanoporous structures constructed by eliminating the second phase

Aside from internal space in the starting nanopower, nanopore could also be creating during the SPS process with a high pressure, high temperature, and high vacuum. Recently, Zou and co-workers succeeded in decomposition of indium selenides (InSe_y) nanoprecipitates in SnSe pellets [31]. In the first step, they induced InSe_y nanoprecipitates in the as-synthesized SnSe matrix of single-crystal microplates via a facile solvothermal method, as shown in Figs. 4(a) and 4(b). Detailed characterizations of the sample indicated that the particle size of InSe_y nanoprecipitates was between 10 and 50 nm (Fig. 4(e)). Due to the decomposition temperatures of InSe, are lower than that of SnSe, the InSe_y particles could decompose to Se and In. In the second step, the SnSe-InSe_y products were sintering to the pellets with nano pores through a SPS process at 950 K (Figs. 4(c) and 4(d)). In the sintering process, most of the Se became liquid and were squeezed out of the pellets, leaving nanopores (with diameters of 30-60 nm) in the pellets due to the decomposition of InSe_y precipitates (Fig. 4(f)). The higher porosity in SnSe pellets possessed a lower thermal conductivity of 0.24 $W \cdot m^{\text{--}1} \cdot K^{\text{--}1}$ which derived from the scattering of phonon

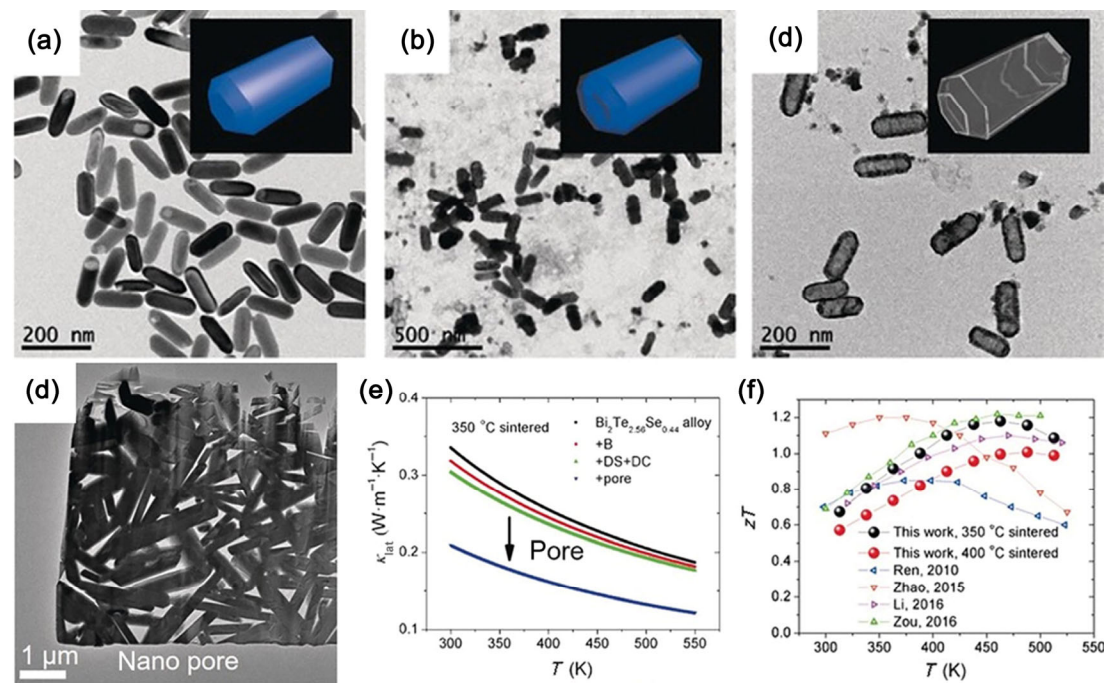


Figure 3 Low-magnification TEM images of (a) Te nanorods (step 1), (b) Te@Bi-Se core-shell nanorods (step 2), and (c) Bi₂Te_{2.5}Se_{0.5} hollow nanorods (step 3). (d) TEM image of the porous Bi_{2.02}Te_{2.56}Se_{0.44} nanocomposite. (e) The effect of nano pores on thermal conductivity. (f) *zT* of the porous nanocomposite in this work compared with previously reported samples. Reproduced with permission from Ref.[30], © Wiley-VCH Verlag GmbH & Co. KGaA, Weinheim 2017.

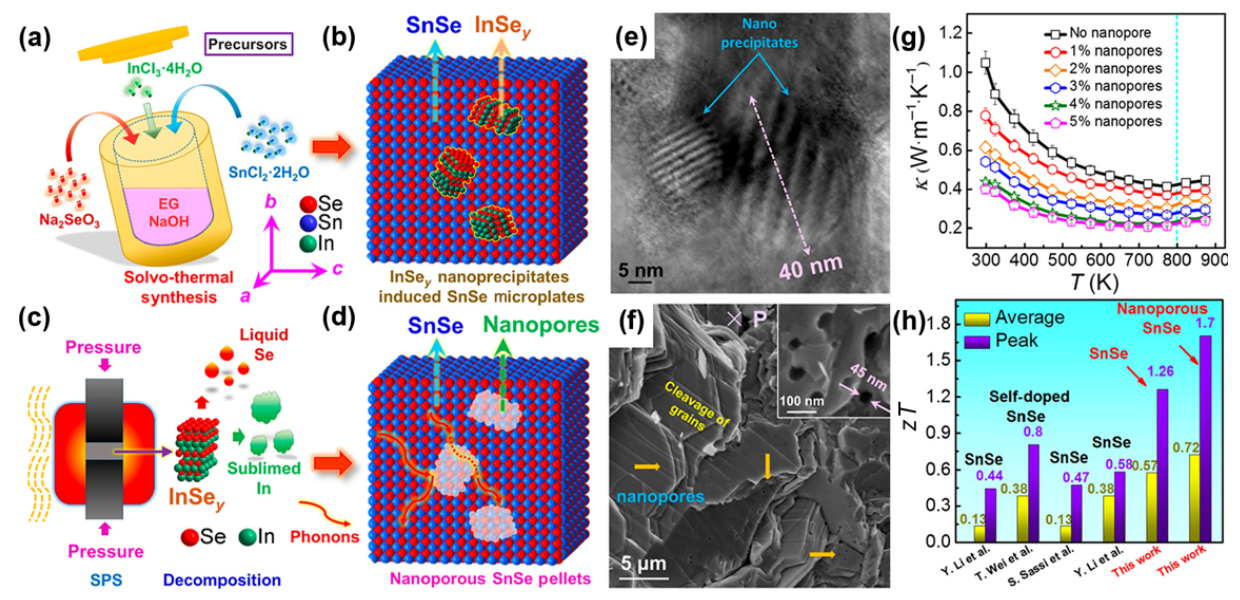


Figure 4 (a)–(d) Illustration of nanoporous design. (e) HRTEM image to show $InSe_y$ nanoprecipitates in SnSe microplates. (f) SEM image with inset of a magnified SEM image of nanopores in the pellets after SPS. (g) Temperature dependence of thermal conductivity. (h) Comparisons of average and peak zT of the nanoporous SnSe pellets with reported SnSe works. Reproduced with permission from Ref. [31], © American Chemical society 2018.

at grain boundaries and interfaces (Fig. 4(g)). An excellent zT of ~ 1.7 at 823 K and a high power factor of 5.06 μ W·cm⁻¹·K⁻² have been achieved (Fig. 4(h)).

4 Micro-scale porosity increases for thermoelectric materials

Afterward, scientists also tried to increase the porosity of thermoelectric materials at microscale level. One feasible method is using irregularly shaped nanostructures as building blocks to construct porous thermoelectric materials. In this method, porosity that arises from the irregular shape and imperfect stacking of building blocks can offer an additional

means to reduce the thermal conductivity [33–35]. The second method is creating microscale pores during the sintering process using a melt-centrifugation method [36]. The third method is constructing three-dimensional (3D) porous hierarchical architectures.

4.1 Tunable spatial packing

At a higher scale level (microscale), tunable spatial packing could also be used to increase porosity. The packing density and porosity of the as-sintered pellet can be tuned through controlling the shape or morphology of the starting nanopowder [9, 37]. For example, Wu and coworkers synthesized PbS nanocrystals with large grain size and controllable shape. They

studied the effect of different packing perfection on their thermal conductivity [34]. Using shape-controlled nanoparticles (hexapod, less-protruding hexapod, and octahedron) as starting materials, the relative density can be regulated with different packing perfection (Fig. 5) [34]. The trend in the porosity after sintering was related to the context of the spatial stacking of the PbS nanoparticles. For the PbS hexapods, it packed in the lowest relative density (82%) which induced the largest portions of pores (18% of porosity). And the relative density of the PbS octahedrons can be as high as 95% (5% of porosity). The higher porosity in the final product resulted in a much lower κ (Fig. 5(g)). Thus, the sample based PbS hexapods with highest porosity exhibited the highest zT of 1.06 at 838 K (Fig. 5(h)). In addition, the studies of density functional theory confirmed that the phonon-pore scattering reduced thermal conductivity, leading to a high figure of merit.

To further explore the effect of spatial packing, Wu and coworkers also tried to use NHSs with sophisticated structure as the starting materials to increase porosity to enhance the thermoelectric performance [35]. In the beginning, PbTe-BiSbTe NHSs were synthesized through a solution-based route. After sintering, the relative density of the obtained bulk structure is 78% which means its high porosity (22%). And the bulk

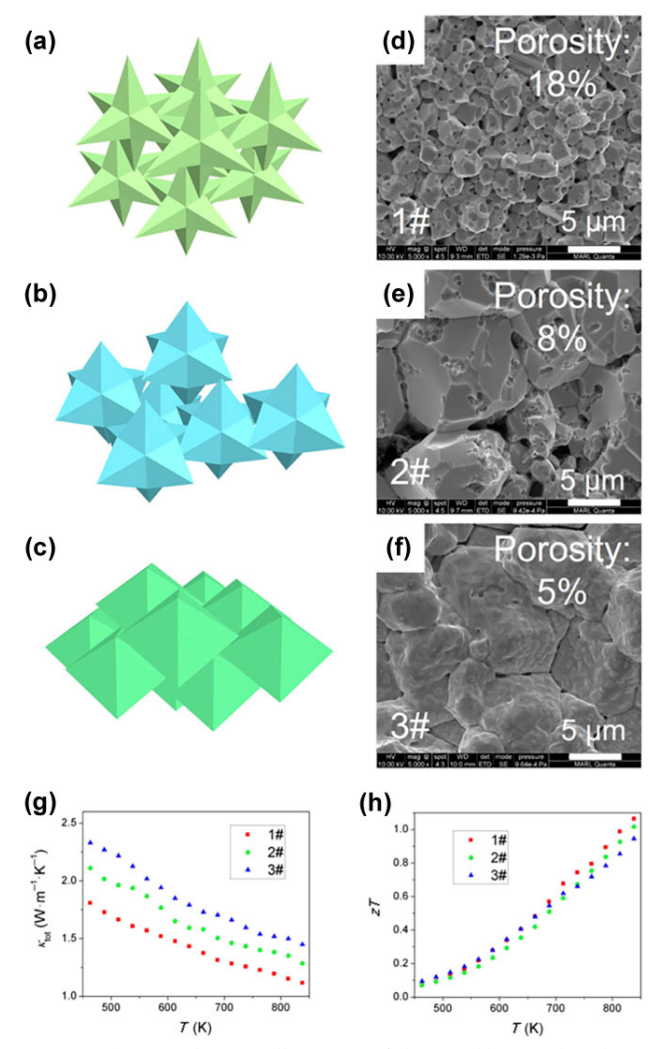


Figure 5 (a)-(c) Schematic illustration of the possible spatial packings of 1# (hexapods), 2# (less-protruding hexapods), and 3# (octahedra), respectively. (d)-(f) SEM images of the as-sintered 1# (from hexapods), 2# (from less-protruding hexapods,) and 3# (from octahedra) samples. Temperature dependence of (g) thermal conductivity and (h) zT of the three samples. Reproduced with permission from Ref. [34], © American Chemical society 2018.

structure showed suppressed thermal conductivity which was determined by the phonons scattering induced by the porous structure. Finally, the zT is higher than 1.0 in the low medium temperature (513-613 K) range. Therefore, using irregularly shaped nanoparticles or NHSs as building blocks could decrease the filling fraction (and relative density) of the assembled pellet to increase the porosity. And this method of tunable spatial packing could be a general approach to increase the porosity of thermoelectric materials.

4.2 Microscale pore induced by unconventional techniques

Aside from creating microscale pores through adjusting packing density, the microscale pores could also be formed using a melt-centrifugation method. Snyder and co-workers synthesized a liquid-fused porous p-type (Bi,Sb)₂Te₃ with a zT value of 1.2 using an unconventional melt-centrifugation technique (Fig. 6) [36]. First, Bi_{0.5}Sb_{1.5}Te_{4.31} and Bi_{0.3}Sb_{1.7}Te_{4.28} were made through high-energy ball milling. Then the ball-milled powders were pressed rapidly to produce pellets through rapid hot press process at 400 °C. Next, the pellet was sealed under vacuum in the silica ampoule and heated to 500 °C. Finally, the ampoule was quickly taken out from the furnace and centrifuged at 4,000 rpm, for 105 s which is exactly the meltcentrifugation process. And this melt-centrifugation process squeezed out the liquid Te (melting point: ≈ 425 °C) from the

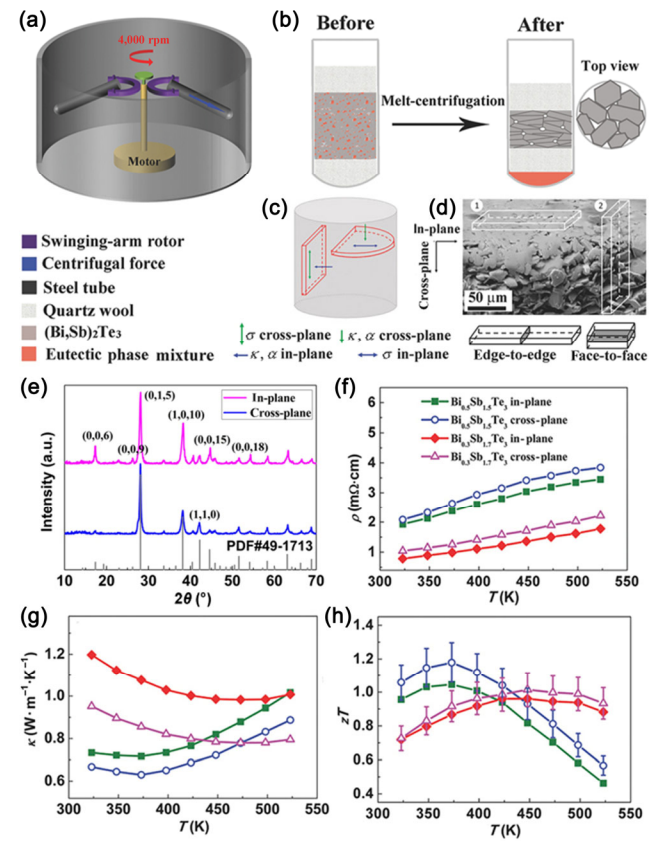


Figure 6 (a) Schematic illustration of centrifugation. (b) Sample in the silica ampoule before and after melt centrifugation. The sample becomes anisotropic and porous after melt centrifugation. (c) Schematic illustration of the measurement direction of thermoelectric transport properties. (d) SEM image of the cross section of one obtained sample. (e) XRD patterns of the centrifuged sample along both in-plane and cross-plane directions. Temperature dependence of (f) resistivity, (g) total thermal conductivity, and (h) zT values of the centrifuged samples in both in-plane and cross-plane directions. Reproduced with permission from Ref. [36], © Wiley-VCH Verlag GmbH & Co. KGaA, Weinheim 2018.

solid (Bi,Sb)₂Te₃ phase under strong centrifugal force. Detailed structural analyses revealed the formation of a porous network with a layered structure (Fig. 6(d)). After the melt-centrifugation process, the thermal conductivity of this porous material sharply decreased due the phonon transport is strongly disrupted. They claimed this microstructure with microscale pores displayed a zT value of 1.2 which was higher than that of conventional Bi_{0.5}Sb_{1.5}Te₃ (a zT value \approx 1). And through Debye–Callaway and effective medium theory modeling, they concluded that the microscale pore structure resulted in as much as a 50% total reduction of thermal conductivity. Furthermore, they also claimed this unconventional melt-centrifugation technique could be a general method for synthesizing high efficiency porous thermoelectric materials.

4.3 3D hierarchical architectures-based carbon nanotubes

Besides the spatial packing and melt-centrifugation methods, 3D hierarchical architectures have also been demonstrated to increase the porosity of thermoelectric materials. Recently, Cho et al. reported a rapid solvent evaporation method to prepare carbon nanotube (CNT) foam with porosity exceeding 90% [38]. The formation of pores in the CNT networks will suppress the lattice thermal conductivity of CNTs and increase the temperature gradient for a high-performance thermoelectric generator. The obtained highly porous CNT shows a much lower thermal conductivity of 0.17 W·m⁻¹·K⁻¹. The electrical conductivity and power factor are 4.02 S·cm⁻¹ and 0.43 μW·m⁻¹·K⁻², relatively. Even though the figure merit of zT is only 7.6×10^{-4} , the thermoelectric performance of CNT foam can be easily enhanced further through doping by molecular dopants, such as FeCl3 and benzyl viologen (BV). Wang et al. also reported a 3D hierarchical architecture based CNTs [39]. They introduced MoS₂ into CNT to form hybrid MoS₂/CNTs 3D hierarchical architectures which could increase electrical conductivity and decrease thermal conductivity. The MoS2/CNTs film shows high electrical conductivity of 235 ± 5 S⋅cm⁻¹ and low thermal conductivity of 19 ± 2 mW·m⁻¹·K⁻¹ which lead to the figure merit of zT of 0.17 at room temperature. These works provide new insights for the design, synthesis, and mechanistic investigation of advanced 3D hierarchical architectures for energy conversion which should be applicable to other materials with challenging structures/properties.

5 Conclusions and perspectives

The engineering of thermoelectric materials offers new directions for thermoelectric research, improving the thermoelectric performance of the existing chemical compositions of thermoelectric materials. Based on the achievements, the thermal conductivity could be significantly reduced by increasing the porosity of thermoelectric materials at different scales, finally leading to a high figure of merit. The thermoelectric performance of recently reported porous structures is summarized in Table 1. The porous structure in thermoelectric materials not only increases the thermoelectric performance but also endows them with better portability due to lower relative mass density. In the meantime, the porous structure might decrease the use of expensive raw materials. We would also like to discuss several prospects of the thermoelectric materials.

First, using hollow nanostructure as a powder precursor should be an effective method to increase the porosity of a thermoelectric material. Considering the hollow materials have been extensively investigated, we can adopt the methods for preparation of hollow nanomaterials to make hollow thermoelectric materials. For example, hard-template method which has been widely used in fabrication of hollow nanomaterials could be used to construct porous thermoelectric materials. Second, new techniques about creating pores in the sintering process should be developed. The aforementioned unconventional methods (such as melt-centrifugation and eliminating the second phase during the sintering) in this review are high efficiency methods and could be employed to create porous thermoelectric structure. However, these two methods are not universal since they required complicated process. Therefore, some universal and simple techniques which could improve porosity are necessary for the industrial applications of porous thermoelectrics. Finally, apart from creating porous structure in only one scale (atomic, nano, or micro), the porosity can be further increased by combining the methods at different scales. For example, if atomic doping was building in a nanoscale hollow structure, the porosity of the structure could be further improved, leading to lower thermal conductivity and a high figure of merit. Except for decreasing the thermal conductivity, the performance of thermoelectric could also be improved by increasing the power factor which is dominated by the electronic band structure of the thermoelectric materials. Therefore, more efforts should be made on developing of nanoheterostructures, multiple-dopant strategy, decoupling interrelated parameters, and so on. And removing the organic ligands on thermoelectric nanostructures could also be an effective method to increase the electrical conductivity and power factor. In this review, the summaries of porous thermoelectric materials are expected to provide a basic understanding of the strategies employed for decreasing the thermal conductivity, which could provide some insights

Table 1 The thermoelectric performance of recently reported porous structures

Porous materials	Porosity	T (K)	$\kappa (W \cdot m^{-1} \cdot K^{-1})$	σ (S·m ⁻¹)	zT	Ref. Year
Bi ₁₃ S ₁₈ I ₂	N/A	788	0.48	~ 10,000	1.0	[25] 2018
$PbBi_{4}Te_{7}$	16%	688	~ 7.2	~ 74,000	0.95	[26] 2018
$Bi_{2.02}Te_{2.56}Se_{0.44} \\$	22.8%	463	~ 0.5	N/A	1.18	[30] 2017
SnSe	3.9%	823	0.24	~ 4,000	~ 1.7	[31] 2018
PbS	18%	838	~ 1.2	~ 41,000	1.06	[34] 2018
PbTe-BiSbTe	22%	513	~ 0.5	~ 28,000	~ 1	[35] 2017
(Bi,Sb) ₂ Te ₃	27%	373	~ 0.65	N/A	1.2	[36] 2018
Porous CNT foam	> 90%	298	~ 0.17	402	7.6×10^{-4}	[38] 2019
MoS ₂ /CNTs	N/A	298	~ 0.019	~ 23,500	0.17	[39] 2020

for the development of other types of porous thermoelectric composites.

Acknowledgements

The work documented is supported under a research grant from the US Navy, Mr. Peter A. Morrison at the Office of Naval Research (Award Number N000141912518) located in Arlington, Virginia, USA. Y. W. also thanks U.S. National Science Foundation for the support under Award Number 1905037.

References

- Xu, B.; Feng, T. L.; Li, Z.; Zheng, W.; Wu, Y. Large-scale, solution-synthesized nanostructured composites for thermoelectric applications. *Adv. Mater.* 2018, 30, 1801904.
- [2] Tan, G. J.; Zhao, L. D.; Kanatzidis, M. G. Rationally designing high-performance bulk thermoelectric materials. *Chem. Rev.* 2016, 116, 12123–12149.
- [3] Sootsman, J. R.; Chung, D. Y.; Kanatzidis, M. G. New and old concepts in thermoelectric materials. *Angew. Chem., Int. Ed.* 2009, 48, 8616–8639.
- [4] Shi, X.-L.; Zou, J.; Chen, Z.-G. Advanced thermoelectric design: From materials and structures to devices. *Chem. Rev.* 2020, 120, 7399–7515
- [5] Zheng, X. F.; Liu, C. X.; Yan, Y. Y.; Wang, Q. A review of thermoelectrics research—Recent developments and potentials for sustainable and renewable energy applications. *Renew. Sustain. Energy Rev.* 2014, 32, 486–503.
- [6] Yang, L.; Chen, Z. G.; Dargusch, M. S.; Zou, J. High performance thermoelectric materials: Progress and their applications. Adv. Energy Mater. 2018, 8, 1701797.
- [7] Satterthwaite, C. B.; Ure, R. W. Jr. Electrical and thermal properties of Bi₂Te₃. *Phys. Rev.* 1957, 108, 1164–1170.
- [8] Dresselhaus, M. S.; Chen, G.; Tang, M. Y.; Yang, R. G.; Lee, H.; Wang, D. Z.; Ren, Z. F.; Fleurial, J. P.; Gogna, P. New directions for low-dimensional thermoelectric materials. *Adv. Mater.* 2007, 19, 1043–1053.
- [9] Son, J. S.; Choi, M. K.; Han, M. K.; Park, K.; Kim, J. Y.; Lim, S. J.; Oh, M.; Kuk, Y.; Park, C.; Kim, S. J. et al. n-Type nanostructured thermoelectric materials prepared from chemically synthesized ultrathin Bi₂Te₃ nanoplates. *Nano Lett.* 2012, 12, 640–647.
- [10] Minnich, A. J.; Dresselhaus, M. S.; Ren, Z. F.; Chen, G. Bulk nanostructured thermoelectric materials: Current research and future prospects. *Energy Environ. Sci.* 2009, 2, 466–479.
- [11] Vineis, C. J.; Shakouri, A.; Majumdar, A.; Kanatzidis, M. G. Nanostructured thermoelectrics: Big efficiency gains from small features. Adv. Mater. 2010, 22, 3970–3980.
- [12] Ohta, H.; Kim, S.; Mune, Y.; Mizoguchi, T.; Nomura, K.; Ohta, S.; Nomura, T.; Nakanishi, Y.; Ikuhara, Y.; Hirano, M. et al. Giant thermoelectric Seebeck coefficient of a two-dimensional electron gas in SrTiO₃. *Nat. Mater.* 2007, 6, 129–134.
- [13] Heremans, J. P. The anharmonicity blacksmith. Nat. Phys. 2015, 11, 990–991.
- [14] Zheng, W.; Xu, B.; Zhou, L.; Zhou, Y. L.; Zheng, H. M.; Sun, C. H.; Shi, E. Z.; Fink, T. D.; Wu, Y. Recent progress in thermoelectric nanocomposites based on solution-synthesized nanoheterostructures. *Nano Res.* 2017, 10, 1498–1509.
- [15] Shi, E. Z.; Cui, S.; Kempf, N.; Xing, Q. F.; Chasapis, T.; Zhu, H. Z.; Li, Z.; Bahk, J. H.; Snyder, G. J.; Zhang, Y. L. et al. Origin of inhomogeneity in spark plasma sintered bismuth antimony telluride thermoelectric nanocomposites. *Nano Res.* 2020, *13*, 1339–1346.
- [16] Hsu, K. F.; Loo, S.; Guo, F.; Chen, W.; Dyck, J. S.; Uher, C.; Hogan, T.; Polychroniadis, E. K.; Kanatzidis, M. G. Cubic AgPb_mSbTe_{2+m}: Bulk thermoelectric materials with high figure of merit. *Science* 2004, 303, 818–821.
- [17] Niemelä, J. P.; Giri, A.; Hopkins, P. E.; Karppinen, M. Ultra-low thermal conductivity in TiO₂:C superlattices. J. Mater. Chem. A

- **2015**, *3*, 11527–11532.
- [18] Yang, J. H.; Yip, H. L.; Jen, A. K. Y. Rational design of advanced thermoelectric materials. Adv. Energy Mater. 2013, 3, 549–565.
- [19] Xiao, C.; Li, Z.; Li, K.; Huang, P. C.; Xie, Y. Decoupling interrelated parameters for designing high performance thermoelectric materials. *Acc. Chem. Res.* 2014, 47, 1287–1295.
- [20] Chae, K.; Kang, S. H.; Choi, S. M.; Kim, D. Y.; Son, Y. W. Enhanced thermoelectric properties in a new silicon crystal Si₂₄ with intrinsic nanoscale porous structure. *Nano Lett.* 2018, 18, 4748–4754
- [21] Ju, H.; Kim, M.; Park, D.; Kim, J. A strategy for low thermal conductivity and enhanced thermoelectric performance in SnSe: Porous SnSe_{1-x}S_x nanosheets. *Chem. Mater.* **2017**, *29*, 3228–3236.
- [22] Giulia, P. Thermoelectric materials: The power of pores. Nat. Rev. Mater. 2017, 2, 17006.
- [23] Jin, R. C.; Chen, G; Pei, J. PbS/PbSe hollow spheres: Solvothermal synthesis, growth mechanism, and thermoelectric transport property. *J. Phys. Chem. C* 2012, *116*, 16207–16216.
- [24] Qiao, J. X.; Zhao, Y.; Jin, Q.; Tan, J.; Kang, S. Q.; Qiu, J. H.; Tai, K. P. Tailoring nanoporous structures in Bi₂Te₃ thin films for improved thermoelectric performance. ACS Appl. Mater. Interfaces 2019, 11, 38075–38083.
- [25] Xu, B.; Feng, T. L.; Agne, M. T.; Tan, Q.; Li, Z.; Imasato, K.; Zhou, L.; Bahk, J. H.; Ruan, X. L.; Snyder, G. J. et al. Manipulating band structure through reconstruction of binary metal sulfide for high-performance thermoelectrics in solution-synthesized nanostructured Bi₁₃S₁₈I₂. Angew. Chem., Int. Ed. 2018, 57, 2413–2418.
- [26] Xu, B.; Feng, T. L.; Li, Z.; Zhou, L.; Pantelides, S. T.; Wu, Y. Creating zipper-like van der Waals gap discontinuity in low-temperatureprocessed nanostructured PbBi_{2n}Te_{1+3n}: Enhanced phonon scattering and improved thermoelectric performance. *Angew. Chem., Int. Ed.* 2018, 57, 10938–10943.
- [27] Islam, S. M.; Malliakas, C. D.; Sarma, D.; Maloney, D. C.; Stoumpos, C. C.; Kontsevoi, O. Y.; Freeman, A. J.; Kanatzidis, M. G. Direct gap semiconductors Pb₂BiS₂I₃, Sn₂BiS₂I₃, and Sn₂BiSI₅. *Chem. Mater.* 2016, 28, 7332–7343.
- [28] Eggenweiler, U.; Keller, E.; Krämer, V.; Petasch, U.; Oppermann, H. On the crystal structure of Bi₁₁Se₁₂Cl₉. Z. Kristallogr. 1999, 214, 264–270.
- [29] Chen, J.; Sun, Q.; Bao, D. Y.; Liu, T. Y.; Liu, W. D.; Liu, C.; Tang, J.; Zhou, D. L.; Yang, L.; Chen, Z. G. Hierarchical structures advance thermoelectric properties of porous n-type β-Ag₂Se. ACS Appl. Mater. Interfaces 2020, 12, 51523–51529.
- [30] Xu, B.; Feng, T. L.; Agne, M. T.; Zhou, L.; Ruan, X. L.; Snyder, G. J.; Wu, Y. Highly porous thermoelectric nanocomposites with low thermal conductivity and high figure of merit from large-scale solution-synthesized Bi₂Te_{2.5}Se_{0.5} hollow nanostructures. *Angew. Chem., Int. Ed.* 2017, 56, 3546–3551.
- [31] Shi, X. L.; Wu, A.; Liu, W. D.; Moshwan, R.; Wang, Y.; Chen, Z. G.; Zou, J. Polycrystalline snse with extraordinary thermoelectric property via nanoporous design. ACS Nano 2018, 12, 11417–11425.
- [32] Zhao, X. B.; Ji, X. H.; Zhang, Y. H.; Zhu, T. J.; Tu, J. P.; Zhang, X. B. Bismuth telluride nanotubes and the effects on the thermoelectric properties of nanotube-containing nanocomposites. *Appl. Phys. Lett.* 2005, 86, 062111.
- [33] Zhang, G. Q.; Fang, H. Y.; Yang, H. R.; Jauregui, L. A.; Chen, Y. P.; Wu, Y. Design principle of telluride-based nanowire heterostructures for potential thermoelectric applications. *Nano Lett.* 2012, 12, 3627–3633.
- [34] Xu, B.; Feng, T. L.; Li, Z.; Pantelides, S. T.; Wu, Y. Constructing highly porous thermoelectric monoliths with high-performance and improved portability from solution-synthesized shape-controlled nanocrystals. *Nano Lett.* 2018, 18, 4034–4039.
- [35] Xu, B.; Agne, M. T.; Feng, T. L.; Chasapis, T. C.; Ruan, X. L.; Zhou, Y. L.; Zheng, H. M.; Bahk, J. H.; Kanatzidis, M. G.; Snyder, G. J. et al. Nanocomposites from solution-synthesized PbTe-BiSbTe nanoheterostructure with unity figure of merit at low-medium temperatures (500–600 K). Adv. Mater. 2017, 29, 1605140.

- [36] Pan, Y.; Aydemir, U.; Grovogui, J. A.; Witting, I. T.; Hanus, R.; Xu, Y. B.; Wu, J. S.; Wu, C. F.; Sun, F. H.; Zhuang, H. L. et al. Melt-centrifuged (Bi,Sb)₂Te₃: Engineering microstructure toward high thermoelectric efficiency. Adv. Mater. 2018, 30, 1802016.
- [37] Han, G.; Popuri, S. R.; Greer, H. F.; Bos, J. W. G.; Zhou, W. Z.; Knox, A. R.; Montecucco, A.; Siviter, J.; Man, E. A.; Macauley, M. et al. Facile surfactant-free synthesis of p-type SnSe nanoplates with exceptional thermoelectric power factors. *Angew. Chem., Int. Ed.* 2016, 55, 6433–6437.
- [38] Lee, M. H.; Kang, Y. H.; Kim, J.; Lee, Y. K.; Cho, S. Y. Freely shapable and 3D porous carbon nanotube foam using rapid solvent evaporation method for flexible thermoelectric power generators. *Adv. Energy Mater.* 2019, 9, 1900914.
- [39] Li, J. H.; Shi, Q. W.; Röhr, J. A.; Wu, H.; Wu, B.; Guo, Y.; Zhang, Q. H.; Hou, C. Y.; Li, Y. G.; Wang, H. Z. Flexible 3D porous MoS₂/CNTs architectures with ZT of 0.17 at room temperature for wearable thermoelectric applications. Adv. Funct. Mater. 2020, 30, 2002508.